

Electron mean free paths for free-electron-like materials

David R. Penn

National Bureau of Standards, Washington, D. C. 20234

(Received 6 August 1975)

Mean free paths for electrons in bulk jellium are calculated for electrons with energies from a few hundred to a few thousand eV and for values of r_s for 1.5 to 5 where r_s is the average distance between valence electrons measured in units of the Bohr radius. Account is taken of exchange and correlation effects in an approximate way. The present theory is compared to previous theories and to experiments on Al, Be, Si, SiO₂, and Al₂O₃, and in most cases the agreement between theory and experiment is quite good.

I. INTRODUCTION

The experimental techniques of photoelectron spectroscopy and Auger-electron spectroscopy are surface sensitive because of the small mean free path λ of electrons escaping from the solid. This quantity determines the average depth beneath the surface probed by these techniques, and must be known accurately for a quantitative understanding of photoemission and Auger experiments.

We present a calculation of the mean free path in the energy range from a few hundred eV to a few thousand eV, and we also give an asymptotic formula for λ valid above a few thousand eV. The calculation is valid for free-electron-like materials. We consider a material to be free-electron-like if its loss function $-\text{Im}[1/\epsilon(q=0, \omega)]$, as determined from characteristic energy-loss experiments or from optical experiments, shows that the predominant loss mechanism is due to well-defined plasmons which have an energy close to the free-electron value, $\omega_p = (4\pi n e^2/m)^{1/2}$. Roughly speaking, materials which are not composed of transition- or noble-metal atoms are free-electron-like for our purposes. For such a material the inelastic mean free path due to valence-band excitations depends only on the energy of the hot electron and on the average electron density, n , of the material which is parameterized by $r_s = (3/4\pi n)^{1/3} \times (1/a_0)$, where a_0 is the Bohr radius. r_s is the average distance between valence electrons in units of a_0 .

Although the primary cause of the electron attenuation is due to the inelastic scattering of the hot electron from the valence electrons via plasmon and electron-hole production the excitation of core electrons must also be considered as it typically reduces the mean free path by about 10% or so.

Previously, Quinn¹ and Kleinman² have calculated the mean free path for Al and Shelton³ has carried out similar calculations of λ as a function of r_s up to hot-electron energies $\epsilon/\epsilon_F \leq 25$, where ϵ_F is the Fermi energy. We present here what we feel is a more accurate calculation than that of previous workers due to inclusion of exchange and

correlation effects and we extend the calculations up to several thousand eV. Scattering due to surface plasmons is neglected; this is reasonable because of the rather large mean free paths at high energies which we are concerned with, and because at the surface there is some compensation between the decrease in bulk-plasmon scattering and the increase in surface-plasmon scattering.

In Sec. II the theories of Quinn and Shelton are reviewed and a more accurate theory is proposed. In Sec. III numerical results are presented for λ as a function of r_s and a comparison is made with the relevant experiments.

II. CALCULATION OF MEAN FREE PATH

Quinn¹ has calculated the mean free path $\lambda_0(k)$ of a hot electron with momentum k in bulk jellium from the relation

$$\lambda_0(k) = \left(\frac{\hbar k}{m}\right) \left(\frac{\hbar}{2|M_I(k)|}\right), \quad (1)$$

where $\hbar k/m$ is the velocity of the electron and $2M_I/\hbar$ is its lifetime due to inelastic scattering from other electrons or from plasmons. In Eq. (1) the imaginary part of the electron self-energy evaluated at energy $\epsilon_k = \hbar^2 k^2/2m$ is given by¹

$$M_I(k) = -\frac{e^2}{2\pi^2} \int \frac{d^3q}{q^2} \text{Im} \frac{1}{\epsilon(q, \epsilon_k - \epsilon_{\mathbf{k}-\mathbf{q}})}, \quad (2)$$

$$\epsilon_k > \epsilon_{\mathbf{k}-\mathbf{q}} > \epsilon_F,$$

where ϵ_F is the Fermi energy and $\text{Im}(1/\epsilon)$ was chosen by Quinn to be the imaginary part of the inverse of the Lindhard dielectric function which we will denote by ϵ^I . It is convenient to rewrite Eq. (2) in the form

$$M_I(k) = \frac{e^2}{2\pi^2} \int_0^{\epsilon_k - \epsilon_F} d(\hbar\omega) \int \frac{d^3q}{q^2} \text{Im} \frac{1}{\epsilon(q, \omega)} \times \delta(\hbar\omega - \epsilon_k + \epsilon_{\mathbf{k}-\mathbf{q}}), \quad (3)$$

which can be transformed to

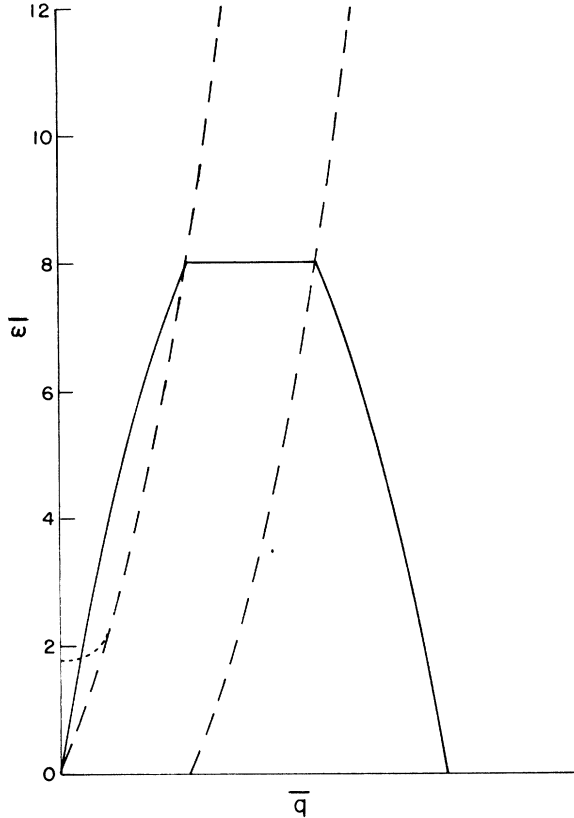


FIG. 1. Region over which $\bar{q}^{-1} \text{Im} \epsilon^{-1}(\bar{q}, \bar{\omega})$ is integrated to obtain M_I in Eq. (4a) is enclosed by the solid line. Its shape depends on the momentum k of the hot electron. $\text{Im} \epsilon^{-1}$ is nonzero between the dashed lines and is singular along the dotted line.

$$\frac{M_I(k)}{\epsilon_F} = \frac{r_s}{\pi a_0 k_F k} \int_0^{k^2-1} d(\bar{h}\bar{\omega}) \int_0^\infty \frac{d\bar{q}}{\bar{q}} \text{Im} \frac{1}{\epsilon(\bar{q}, \bar{\omega})}, \quad (4a)$$

$$2\bar{q}\bar{k} - \bar{q}^2 \geq \bar{h}\bar{\omega},$$

where

$$\bar{k} = k/k_F, \quad (4b)$$

$$\bar{q} = q/k_F, \quad (4c)$$

$$\bar{h}\bar{\omega} = \hbar\omega/\epsilon_F, \quad (4d)$$

and k_F is the Fermi momentum.

The region in $\bar{q}, \bar{\omega}$ space covered by the integration in Eq. (4a) is shown in Fig. 1 as the area bounded by the solid curve. The region bounded by the dashed curves is that for which $\text{Im}[1/\epsilon(\bar{q}, \bar{\omega})] \neq 0$ and represents the portion of $\bar{q}, \bar{\omega}$ space in which an electron can lose momentum \bar{q} and energy $\bar{h}\bar{\omega}$ to another electron, i. e., electron-hole excitation. If the point $(\bar{q}, \bar{\omega})$ lies outside this region the collision process will not be energy and momentum conserving. The dotted curve is the line along which $\text{Im} 1/\epsilon(\bar{q}, \bar{\omega})$ is singular due to the neglect of plasmon damping and corresponds to a process in

which an electron can lose momentum \bar{q} and energy $\bar{h}\bar{\omega}_p(q)$ to a plasmon, the plasmon dispersion relation being $\bar{h}\bar{\omega} = \bar{h}\bar{\omega}_p(\bar{q})$. The plasmon contribution to M_I is obtained by integrating over the line $\bar{\omega} = \bar{\omega}_p(\bar{q})$ as indicated in Eq. (4a) and this contribution to M_I can be approximated by an analytic expression¹; however no corresponding analytic expression has been derived for the electron-hole contribution to M_I which can be a significant fraction of the total self-energy.

Quinn¹ and later other authors² have evaluated λ_0 of Eq. (1) for hot electron energies ϵ_h such that $\epsilon_h/\epsilon_F \leq 25$ and we have extended the calculation up to $\epsilon_h \sim 2 \times 10^3$ eV by evaluating Eq. (4a) numerically and using the results in Eq. (1). Figure 2 shows λ_0 as a function of the hot electron energy ϵ_h for $r_s = 1.5, 2, 3, 4,$ and 5 .

As noted by Shelton³ and by Lundqvist,⁴ $\lambda_0(k)$ in Eq. (1) for the mean free path should be replaced by

$$\lambda_1(k) = \left(\frac{1}{\hbar} \frac{\partial E(k)}{\partial k} \right) \left(\frac{\hbar}{2|\Gamma(k)|} \right), \quad (5)$$

where $E(k)$ and $\Gamma(k)$ are the real and imaginary parts of the energy of an electron with momentum k . The electron velocity is $(1/\hbar) \partial E/\partial k$ and the electron life time is $2\Gamma/\hbar$. E and Γ are determined by

$$E(k) + i\Gamma(k) = \epsilon_h + M_k[E(k) + i\Gamma(k)], \quad (6)$$

where the self-energy M_k is

$$M_k(\epsilon) = \frac{e^2}{2\pi^3} \int_0^{\epsilon - \epsilon_F} d(\hbar\omega) \times \int \frac{dq^3}{q^2} \frac{1}{\epsilon(q, \omega)} \frac{1}{\epsilon - \hbar\omega - \epsilon_{\bar{k}-\bar{q}} + i0^+}. \quad (7)$$

The quantity $M_I(k)$ appearing in Eq. (1) is related to $M_k(\epsilon)$ by

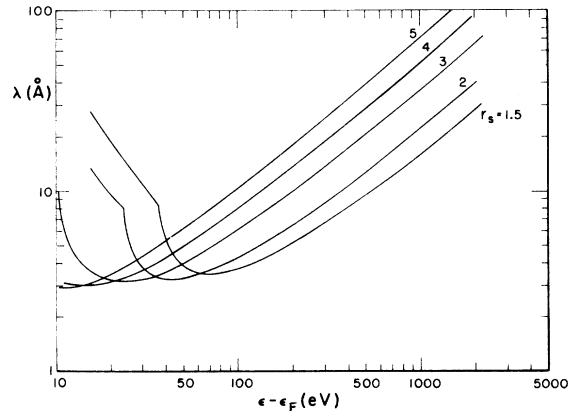


FIG. 2. Mean free path calculated according to the Quinn theory vs the hot-electron energy measured with respect to the Fermi energy as a function of the parameter r_s .

$$M_I(k) = \text{Im} M_k(\epsilon_k). \quad (8)$$

In the limit that the electron-electron interaction is weak, Eqs. (6) and (7) would give $E(k) \rightarrow \epsilon(k)$ and $\Gamma(k) \rightarrow M_I(k)$. Equations (6) and (7) for the mean free path reduce to those used by Quinn only if $M_I(k) \sim \Gamma(k)$, which is not true except for very large values of k . Equation (6) can be solved approximately for $E(k)$ and $\Gamma(k)$ to obtain⁴

$$E(k) + i\Gamma(k) = \epsilon_0 + \epsilon_k + Z(k) [M_k(\epsilon_k) - \epsilon_0], \quad (9a)$$

$$\epsilon_0 = M_{k_F}(\epsilon_{k_F}), \quad (9b)$$

$$Z(k) = \left(1 - \frac{\partial M_k(\epsilon)}{\partial \epsilon} \Big|_{\epsilon=\epsilon_k} \right)^{-1}. \quad (9c)$$

Lundqvist⁵ chose $\epsilon(q, \omega) = \epsilon^L(q, \omega)$ in Eq. (7) and then determined $E(k)$, $\Gamma(k)$, and $Z(k)$ from Eq. (9). Shelton³ used Lundqvist's results to obtain $\lambda_1(k)$ from Eq. (5) and the resulting values of λ_1 differ from those obtained by Quinn from Eqs. (1) and (2) by roughly (5–20%) depending on r_s and on k . As in the cases studied by Quinn, Shelton restricted himself to energies such that $\epsilon_k/\epsilon_F \leq 25$.

Equation (7) for the self-energy $M_k(\epsilon)$ is of course an approximation to the true self-energy \mathfrak{M} which is determined from the system of equations

$$\mathfrak{G} = g + g \mathfrak{M} \mathfrak{G}, \quad (10a)$$

$$\mathfrak{M} = \mathfrak{G} \Gamma V, \quad (10b)$$

$$V = v/\epsilon = v/(1 - vP), \quad (10c)$$

$$P = \mathfrak{G} \Gamma \mathfrak{G}, \quad (10d)$$

where $\langle k | g | k \rangle = (\epsilon - \epsilon_k)^{-1}$ and $\langle k | \mathfrak{G} | k \rangle = (\epsilon - \epsilon_k - \langle k | \mathfrak{M} | k \rangle)^{-1}$ are the one-electron Green's functions in the absence and presence of the Coulomb interaction v . \mathfrak{M} is the self-energy, v is the effective electron-electron interaction, and Γ is the vertex correction. Equation (7) is obtained from Eq. (10) by setting $\Gamma=1$ and $\mathfrak{G}=g$ in (10b). Shelton used $\epsilon = \epsilon^L$ in Eq. (7) which corresponds to setting $\Gamma=1$ and $\mathfrak{G}=g$ in Eq. (10d) as well as in Eq. (10b). We next obtain a more accurate result for \mathfrak{M} by using in Eq. (7) in place of ϵ^L a dielectric function which includes the effects of exchange and correlation. Singwi *et al.*⁶ have developed a theory of the dielectric function which includes the effects of exchange and correlation but their theory does not yield a particularly tractable form for the dielectric function. We therefore turn to a simplified theory of electron correlation developed by Overhauser.⁷ The theory employs a one-mode excitation spectrum; the excitations of the electron gas which consist of plasmons and electron-hole pairs are approximated by a single mode with a plasmon-like excitation spectrum.⁴ In other words, the region in Fig. 1 between the dashed lines as well

as the plasmon line (dotted line) are replaced by a single line. The one-mode formulation as restated by Gersten and Tzoar⁸ is as follows. The one-mode approximation is expressed by

$$\text{Im}[1/\epsilon(q, \omega)] = \lambda_q \delta(\omega - \omega_q), \quad (11)$$

where λ_q is determined from the sum rule

$$\int d\omega \omega \text{Im} \frac{1}{\epsilon(q, \omega)} = -\frac{1}{2} \pi \omega_p^2, \quad (12)$$

where ω_p is the plasma frequency for the electron gas, $\omega_p^2 = 4\pi n e^2/m$. Use of (11) in (12) gives

$$\lambda_q = -\frac{1}{2} \pi \omega_p^2 / \omega_q. \quad (13)$$

The Kramers-Kronig dispersion relation is

$$\text{Re} \frac{1}{\epsilon(q, \omega)} = 1 + \frac{2}{\pi} P \int_0^\infty d\omega' \frac{\omega'}{\omega'^2 - \omega^2} \text{Im} \frac{1}{\epsilon(q, \omega')}, \quad (14)$$

and use of (11) and (13) in (14) gives

$$\text{Re}[1/\epsilon(q, \omega)] = 1 - \omega_p^2 / (\omega_q^2 - \omega^2). \quad (15)$$

In the limit $\omega \rightarrow 0$, Eq. (15) gives

$$\omega_q^2 = \omega_p^2 \epsilon(q, 0) / [\epsilon(q, 0) - 1]. \quad (16)$$

Consequently $\epsilon(q, 0)$ determines all the quantities of interest in the one-mode model.

Although the correct dielectric function $\epsilon_q \equiv \epsilon(q, 0)$ is not known the effects of exchange and correlation on $\epsilon(q, 0)$ can be approximated by assuming that the exchange and correlation potentials are local. Overhauser⁷ then found that

$$\epsilon_q = 1 + (\epsilon_q^0 - 1) / [1 - G(q) (\epsilon_q^0 - 1)], \quad (17)$$

where ϵ_q^0 is the dielectric function in the absence of exchange and correlation and $G(q)$ is related to the exchange and correlation potentials. Overhauser chose $G(q)$ to be such that the correlation energy predicted by the one-mode model agrees with that calculated by Singwi⁶ and also such that ϵ_q given by Eq. (17) agrees with estimates obtained by other workers in the limits $q \rightarrow 0$ and $q \rightarrow \infty$;

$$G(\bar{q}) = 0.275 \bar{q}^2 / (1 + 2.5 \bar{q}^2 + 0.09375 \bar{q}^4)^{1/2}. \quad (18)$$

In the absence of exchange and correlation the electron-plasmon coupling constant in this model is⁹

$$M_q = (e^2 \hbar \omega_p^2 / 2 q^2 \omega_q)^{1/2}, \quad (19)$$

while in the presence of exchange and correlation the coupling constant is given by⁷

$$M_q' = M_q [1 - G(q)]. \quad (20)$$

The electron self-energy in the one-mode model is obtained from⁴ Eq. (7):

$$M'_k(\epsilon) = M_{\text{HF}}(k) + \frac{\hbar}{(2\pi)^4} \int d\omega \int d^3q M_q'^2 \frac{2\hbar\omega_q}{(\hbar\omega)^2 - (\hbar\omega_q)^2 + i0^+} \frac{1}{\epsilon - \hbar\omega - \epsilon_{k-q} - i0^+}, \quad (21a)$$

where M_{HF} is the Hartree-Fock exchange energy

$$M_{\text{HF}}(k) = -\frac{\hbar^2 k_F}{\pi m a_0} \left(1 + \frac{k_F^2 - k^2}{2k k_F} \ln \left| \frac{k_F + k}{k_F - k} \right| \right), \quad (21b)$$

and ω_q is obtained from the use of Eqs. (18) and (17) in Eq. (16). Equation (21a) is integrated to obtain⁴

$$\begin{aligned} M'_k(\epsilon) = & M_{\text{HF}}(k) + \frac{(\hbar\omega_p)^2}{2\pi a_0 k} \left[\int_0^{k-k_F} \frac{dq}{q \hbar\omega_q} [1 - G(q)]^2 \left(\ln \left| \frac{\epsilon_k - \epsilon + \hbar\omega_q}{\epsilon_{k-q} - \epsilon + \hbar\omega_q} \right| - \pi i \Theta(\epsilon_{k+q} - \epsilon + \hbar\omega_q) \Theta(\epsilon - \hbar\omega_q - \epsilon_{k-q}) \right) \right. \\ & + \int_{k-k_F}^{k+k_F} \frac{dq}{q \hbar\omega_q} [1 - G(q)]^2 \left(\ln \left| \frac{(\epsilon_F - \epsilon - \hbar\omega_q)(\epsilon_{k+q} - \epsilon + \hbar\omega_q)}{(\epsilon_F - \epsilon + \hbar\omega_q)(\epsilon_{k-q} - \epsilon - \hbar\omega_q)} \right| - \pi i \Theta(\epsilon_{k+q} - \epsilon + \hbar\omega_q) \Theta(\epsilon - \hbar\omega_q - \epsilon_F) \right) \\ & \left. + \int_{k+k_F}^{\infty} \frac{dq}{q \hbar\omega_q} [1 - G(q)]^2 \left(\ln \left| \frac{\epsilon_k - \epsilon - \hbar\omega_q}{\epsilon_{k-q} - \epsilon + \hbar\omega_q} \right| - \pi i \Theta(\epsilon_{k-q} - \epsilon + \hbar\omega_q) \Theta(\epsilon - \hbar\omega_q - \epsilon_{k-q}) \right) \right], \quad (22) \end{aligned}$$

where $\Theta(x) = 1$ if $x > 0$ and $\Theta(x) = 0$ if $x < 0$. We have retained only those terms in Eq. (22) which are non zero for $\epsilon \sim \epsilon_k$ because M'_k is to be used in Eq. (9).

In order to estimate the accuracy of the one-mode model for energy-loss calculations we calculate λ_0 from Eqs. (1) and (2); but rather than using the Lindhard dielectric function in the term $\text{Im}[1/\epsilon(q, \omega)]$ of Eq. (2) we use the approximation given by Eqs. (11) and (13),

$$\text{Im}[1/\epsilon(q, \omega)] = -\frac{1}{2} \pi (\omega_p^2 / \omega_q) \delta(\omega - \omega_q), \quad (23)$$

where ω_q is determined from Eq. (16) and the quantity $\epsilon(q, 0)$ appearing in (16) is taken to be the Lindhard function $\epsilon^L(q, 0)$. The resulting values for λ_0 differ from those obtained by using the $\epsilon^L(q, \omega)$ directly in Eq. (2) by typically 5%. A somewhat different form for $\epsilon(q, 0)$ has been suggested by Lundqvist⁴ and its use in Eq. (16) gives

$$\omega_q^2 = \omega_p^2 + \frac{1}{3} (\hbar k_F / m)^2 q^2 + (\hbar q^2 / 2m)^2. \quad (24)$$

This describes the electron-hole excitations for large q and leads to an expression for $\epsilon(q, 0)$ via Eq. (16) which gives Fermi-Thomas screening in the limit $q \rightarrow 0$. Equation (24) provides an expression for $\text{Im}[1/\epsilon(q, \omega)]$ via Eqs. (11) and (13). Because of the simple form of Eq. (24) the integral in Eq. (2) can be done analytically and the result inserted in Eq. (1) to obtain

$$\lambda(k) = 2.24 \bar{k}^2 r_s^{-1/2} [\ln g(\bar{q}_1) / g(\bar{q}_2)]^{-1}, \quad (25a)$$

where λ is in angstroms and

$$g(\bar{q}) = \ln \left(\frac{\bar{\omega}_q + \bar{\omega}_p}{\bar{q}^2} + \frac{2}{3\omega_p} \right), \quad (25b)$$

where $\bar{\omega}_p = \hbar\omega_p / \epsilon_F$, $\bar{q} = q / k_F$, and

$$\bar{\omega}_q = (\bar{\omega}_p^2 + \frac{1}{3} \bar{q}^2 + \bar{q}^4)^{1/2}, \quad (25c)$$

and \bar{q}_1 is determined by the equation

$$\bar{\omega}_q = 2\bar{k} \bar{q}_1 - \bar{q}_1^2, \quad (25d)$$

which has the approximate solution

$$\bar{q}_1^2 \approx \bar{\omega}_p^2 / (4\bar{k}^2 - \frac{4}{3} - 2\bar{\omega}_p), \quad (25e)$$

and \bar{q}_2 is determined by

$$\bar{\omega}_q = \bar{k}^2 - 1, \quad (25f)$$

which has the solution

$$\bar{q}_2^2 = -\frac{2}{3} + \left[\left(\frac{2}{3} \right)^2 + (\bar{k}^2 - 1)^2 - \bar{\omega}_p^2 \right]^{1/2}. \quad (25g)$$

The mean free path given by Eq. (25a) differs from that obtained in the Quinn theory (which uses $\text{Im}[1/\epsilon^L(q, \omega)]$ in Eq. (2)) by less than 1% for hot electrons with sufficiently high energies; $\epsilon_k / \epsilon_F \geq 9$. Thus the Quinn results for the mean free part of a hot electron can be obtained almost exactly from the Lundqvist version of the one-mode model as specified by Eq. (24). The reason for this is not clear at present.

Eliminating $\epsilon(q, 0) \equiv \epsilon_q$ from Eqs. (16) and (17) gives

$$\omega_q^2 = \omega_p^2 \left[\left(\frac{\epsilon_q^0}{\epsilon_q^0 - 1} \right) - G(q) \right] = (\omega_q^0)^2 - \omega_p^2 G(q), \quad (26)$$

where ω_q^0 is the one-mode dispersion relation that obtains in the absence of exchange and correlation. We now combine Lundqvist's version of the one-mode model, Eq. (24), with Overhauser's treatment of correlation and exchange, Eq. (17), to obtain

$$\omega_q^2 = \omega_p^2 [1 - G(q)] + \frac{1}{3} (\hbar k_F / m)^2 q^2 + (\hbar q^2 / 2m)^2. \quad (27)$$

We use Eq. (27) in Eq. (22) to obtain $M'_k(\epsilon)$ and then the mean free path λ is found from Eqs. (9) and (5). As stated above, in the case $G(q) = 0$ determining the mean free path from Eqs. (1) and (2) gives values for λ which agree with the Quinn theory to within 1% for $\epsilon_k / \epsilon_F \geq 9$, where ϵ_k is the energy of the hot electron. The calculation carried out by Shelton³ is essentially equivalent to taking $G = 0$ in

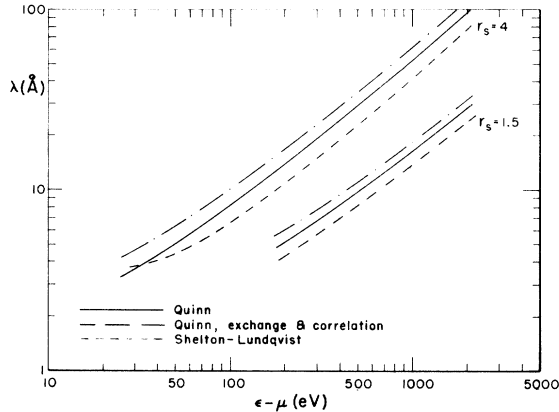


FIG. 3. Comparison of the mean free paths calculated via the theories of Quinn, Shelton and Lundqvist, and Quinn with correlation and exchange.

Eqs. (26) and (20) and then determining λ from Eqs. (21), (9), and (5).

III. NUMERICAL RESULTS AND COMPARISON WITH EXPERIMENT

A. Numerical results

In this section we discuss the results of (a) extending the Shelton-Lundqvist theory of the mean free path to higher energies by solving the system of Eqs. (5), (6), and (22) and using the Lundqvist version of the one-mode theory, Eq. (24), to determine ω_q and ϵ_q ; (b) including exchange and correlation in the Quinn theory of the mean free path by solving the system of Eqs. (1) and (22) and using the one-mode theory as specified by Eq. (27) to determine ω_q and ϵ_q ; (c) determining a "best" estimate of the mean free path by including some of the effects of exchange and correlation on the Shelton-Lundqvist theory [Eqs. (5), (6), and (22)] by using the one-mode theory as specified by Eq. (26) to determine ω_q and ϵ_q . The main purpose in presenting the results of (a) and (b) above is to separate the effects of the corrections to the Quinn theory included in (c). Finally, the results of (c) will be compared to experimental measurements of the mean free path in Al, Al₂O₃, Be, Si, and SiO₂.

The results of (a) for the mean free path as a function of energy for $r_s = 1.5$ and $r_s = 4$ are shown in Fig. 3. The calculation is restricted to values of energy such that $\epsilon/\epsilon_F > 9$ because, as discussed in Sec. II, it is for these values that the Lundqvist version of the one-mode theory reproduces the "Quinn" theory of Fig. 2 to an accuracy of better than 1%. Figure 3 shows that the mean free paths calculated in the Shelton-Lundqvist theory are (10–25%) smaller than those given by the Quinn theory for $\epsilon > 200$ eV, we find $[(1/\hbar)(\partial E/\partial k) - \hbar k/m]/(\hbar k/m)$ is less than 3% for the values of r_s con-

sidered and for $\epsilon = 2000$ eV it is less than $\frac{1}{2}\%$ so the difference between the two theories comes about because of the difference between Γ and M . The origin of this difference can be understood by examining the asymptotic k dependence of the quantities $Z(k)$ and $M_k(\epsilon_k)$ which determine Γ via Eq. (9).

It follows trivially from Eq. (22) that for large k

$$M_I(k) \equiv \text{Im } M_k(\epsilon_k) \simeq -\alpha(\ln \bar{k} + \beta)/\bar{k}, \quad (28a)$$

$$\text{Re } M_k(\epsilon_k) \simeq -\delta/\bar{k}, \quad (28b)$$

$$\text{Re } Z(k) \simeq 1, \quad (28c)$$

$$\text{Im } Z(k) \simeq -\gamma/\bar{k}, \quad (28d)$$

where α , β , δ , and γ are constants that depend on r_s and on the explicit form of ω_q and $G(q)$. Use of Eq. (28) in Eq. (9) gives for large k

$$E(k) \simeq \epsilon_0 + \epsilon_k, \quad (29a)$$

$$\Gamma(k) \simeq -\alpha(\ln \bar{k} + \beta - \gamma\epsilon_0)/\bar{k}, \quad (29b)$$

and use of Eq. (28) in Eq. (5) yields

$$\lambda(k) \simeq (0.276 r_s / \alpha) \bar{k}^2 / (\ln \bar{k} + \phi), \quad (30a)$$

$$\phi = \beta - \gamma\epsilon_0, \quad (30b)$$

for the asymptotic form of the Shelton-Lundqvist mean free path. Equation (28a) and Eq. (1) show that the Quinn mean free path also has the form (30a) with $\phi = \beta$. Values of α and ϕ as functions of r_s are given in Table I for the Quinn theory and the Shelton-Lundqvist theory, (a).¹⁰ Because $-\gamma\epsilon_0$ as well as β in (30c) are positive the Quinn mean free path is longer than the Shelton-Lundqvist mean free path.

The results of (b), including exchange and correlation effects in the Quinn theory, for the mean free path as a function of energy are shown in Fig. 3 for $r_s = 1.5$ and 4. It is seen that the effect of including exchange and correlation in the Quinn theory lengthens the mean free path by (10%–20%). The effect of correlation and exchange is to weaken the effective electron-electron interaction and this naturally implies longer mean free paths. For

TABLE I. Values of α and ϕ that determine the asymptotic form of the mean free path for various theories. In all the theories, $\alpha = 0.246 r_s^{3/2}$ and in the Quinn theory $\phi = -\frac{1}{2} \ln(\frac{1}{12} + \frac{1}{8} \bar{\omega}_p)$.

r_s	Quinn		Shelton-Lundqvist ^a		Quinn ^b	
	α	ϕ	α	ϕ	α	ϕ
1.5	0.45	0.74	0.45	1.1	0.45	0.41
2	0.70	0.69	0.70	1.2	0.70	0.34
3	1.3	0.62	1.3	1.4	1.3	0.23
4	2.0	0.57	2.0	1.5	2.0	0.14

$$\lambda (\text{\AA}) = 0.276 r_s \bar{k}^2 / [\alpha (\ln \bar{k} + \phi)]$$

^aNo exchange or correlation.

^bIncludes exchange and correlation.

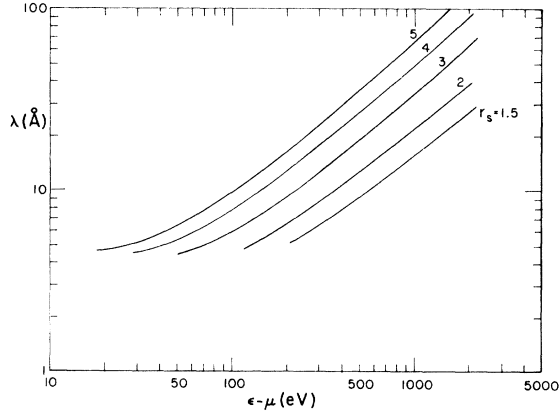


FIG. 4. Mean free path vs hot-electron energy measured with respect to the Fermi energy as determined by the "best" theory (see text).

large k , $M_I(k)$ is given by Eq. (28a) and $\lambda(k)$ by Eq. (30a) with α and $\phi = \beta$ given in Table I.

Finally, the results of (c), the "best" estimate for the mean free path, are shown in Fig. 4. The corrections to the Quinn theory considered in (a) and (b) tend to cancel and the resulting mean free paths of Fig. 4 are lower than those given by the Quinn theory (Fig. 2) by at most 10% and typically 5%. For large k , Eqs. (28)–(30) are valid and the quantities α , ϕ , ϵ_0 , γ , and δ are given in Table II as functions of r_s .

Because the corrections to the Quinn theory turn out to be fairly small and because the Lundqvist version of the one-mode model reproduces the Quinn theory to better than 1% we expect that the results of (c) given in Fig. 4 are quite reliable within the context of the approximations $\Gamma \sim 1$ and $S \sim g$ made in Eq. (10b). It is difficult to assess the errors made in those approximations.

We expect the results for the mean free path depicted in Fig. 4 to be valid for materials which are nearly-free-electron-like. As a rough crite-

TABLE II. Values of parameters for the "best" theory that determine the asymptotic form of the mean free path and other quantities of interest.

r_s	α	ϕ	β	ϵ_0	γ	δ
1.5	0.45	0.89	0.41	-0.56	0.72	0.39
2	0.70	0.91	0.34	-0.76	1.1	0.52
3	1.3	0.95	0.23	-1.2	2.0	0.78
4	2.0	1.0	0.14	-1.6	3.1	1.04
5	2.8	1.1	0.081	-2.1	4.3	1.3

$$\lambda(\text{\AA}) = 0.276 r_s \bar{k}^2 / [\alpha (\ln \bar{k} + \phi)]$$

$$M_R/\epsilon_F = -\delta/\bar{k}, \quad M_I/\epsilon_F = -\alpha (\ln \bar{k} + \beta)$$

$$Z_R = 1, \quad Z_I = \gamma/\bar{k}$$

TABLE III. Values of A , ρ , N , and ΔE used to estimate λ_c , the mean free path due to core excitations. The values of ΔE are crude estimates but are sufficient because $\lambda_c \gg \lambda$.

	A	ρ	N	ΔE
Al	26.98	2.7	8	150
Be	9.012	1.85	2	150
Si	28.09	2.42	8	160
SiO ₂	60.06	2.3	8	160
Al ₂ O ₃	102.0	3.7	16	150

$$\lambda_c(\epsilon) = \frac{2.55 \times 10^{-3} A \epsilon}{\rho(N/\Delta E) \ln(4\epsilon/\Delta E)}$$

ri- on we assume that a material is free-electron-like if its $q=0$ loss function, $-\text{Im}[1/\epsilon(0, \omega)]$ as determined from characteristic energy-loss experiments¹¹ or from optical experiments¹¹ indicates that the primary loss mechanism is due to well-defined plasmon excitations which have an energy that is reasonably close to the free electron value, $\omega_p = (4\pi n e^2/m)^{1/2}$. As a rough rule of thumb, most materials which are not composed of transition-metal or noble-metal atoms fit into this category.

B. Comparison with experiment

The status of experimentally determined mean-free-path measurements has been reviewed by Powell.^{12,13} As discussed by Powell the experiments are difficult and tedious and it is not easy to determine their accuracy. We will only refer to those experiments in which the mean free path has been measured for several values of hot-electron energy by one investigator. Such experi-

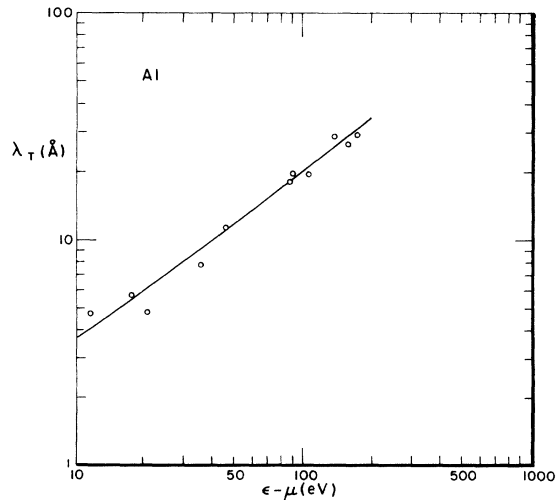


FIG. 5. Total mean free path for Al including inelastic scattering by both valence and core electrons is denoted by the solid line. The experimental points are due to Tracy.

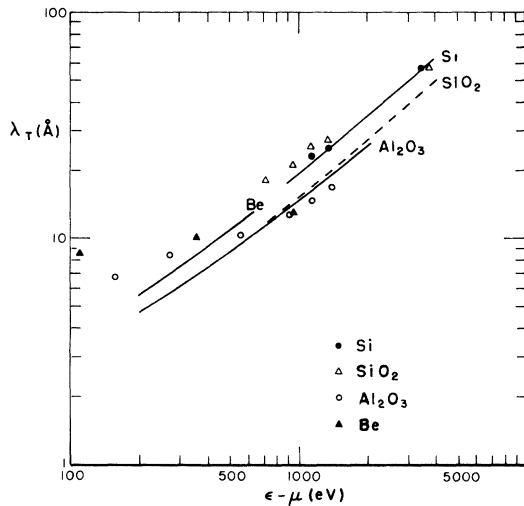


FIG. 6. Total mean free paths for Be (Ref. 15), Si (Ref. 16), SiO₂ (Ref. 16), Al₂O₃ (Ref. 17), are compared to experimentally determined points.

ments on free-electron-like materials have been carried out on Al,¹⁴ Be,¹⁵ Si,¹⁶ SiO₂,¹⁶ and Al₂O₃.¹⁷

The theory discussed in Sec. II is incomplete in the sense that it neglects the inelastic scattering of hot electrons by the core electrons of the material under consideration. Powell¹² has worked out a theory of this effect and finds

$$\lambda_c(\epsilon_k) \approx 2.55 \times 10^{-3} \epsilon_k A / \rho \sum_i \frac{N_i}{\Delta E_i} \ln \frac{4\epsilon_k}{\Delta E_i} \text{ (\AA)}, \quad (31)$$

where ϵ_k is the energy of the hot electron, A is the atomic (or molecular) weight of the component atoms or molecules of the material, ρ is the density, and ΔE_i is the average characteristic energy loss associated with the N_i core electrons. Equation (31) can also be used to calculate λ due to the valence electrons; however, it leaves out the contribution to λ from electron-hole excitations. The effective mean free path λ_T is given by

$$1/\lambda_T = 1/\lambda_c + 1/\lambda, \quad (32)$$

where λ is the mean free path due to the valence electrons and given in Fig. 4. Typically λ_T is smaller than λ by roughly 10%. Values of A , ρ , N_i , and ΔE_i used in Eq. (31) are given in Table III for Al, Be, Si, SiO₂, and Al₂O₃. λ_T as determined from Fig. 4 and Eqs. (31) and (32) for Al is shown in Fig. 5 as are the experimentally determined points.¹⁴ The agreement between theory and experiment is excellent; however, this must be in part fortuitous since the agreement is far better than could possibly be expected due to the uncertainties in both the theory and the experiment. In Fig. 6 we compare the results of the theory, including core excitations, with the experimental results for Be, Si, SiO₂, and Al₂O₃. The agreement is reasonable in all cases except SiO₂.

¹J. J. Quinn, Phys. Rev. **126**, 1453 (1962).

²L. Kleinman, Phys. Rev. B **3**, 2982 (1971).

³J. C. Shelton, Surf. Sci. **44**, 305 (1974).

⁴B. I. Lundqvist, Phys. Kondens. Mater. **6**, 206 (1967).

⁵B. I. Lundqvist, Phys. Status Solidi **32**, 273 (1969).

⁶K. S. Singwi, M. P. Tosi, and R. H. Land, Phys. Rev. **176**, 589 (1968).

⁷A. W. Overhauser, Phys. Rev. **83**, 1888 (1971).

⁸J. I. Gersten and N. Tzoar, Phys. Rev. B **8**, 5671 (1973).

⁹D. F. Dubois, Ann. Phys. (N.Y.) **7**, 174; **8**, 24 (1959).

¹⁰ $\epsilon_0 = M_{k_F}(\epsilon_{k_F})$ as calculated by the one-mode model agrees with the value given by Ref. 5 to an accuracy of 3% or

better for $r_s = 2, 3, 4$, and 5 which are the cases considered in Ref. 5.

¹¹For a review of the field see D. Pines, *Elementary Excitations in Solids* (Benjamin, New York, 1963).

¹²C. J. Powell, Surf. Sci. **44**, 29 (1974).

¹³C. J. Powell, Rev. Mod. Phys. (to be published).

¹⁴J. C. Tracy, J. Vac. Sci. Technol. **11**, 280 (1974).

¹⁵M. P. Seab, Surf. Sci. **32**, 703 (1972).

¹⁶R. Flitsch and S. I. Raider, J. Vac. Sci. Technol. **12**, 305 (1975).

¹⁷F. L. Battye, J. G. Jenkin, J. Liesegang, and R. C. G. Leckey, Phys. Rev. B **9**, 2887 (1974).